Nr 10 (501–556) PAŹDZIERNIK 2021 Tom LXVI

POLIMERY

Acrylic polyurethane coatings durability under outdoor weathering in an industrial area

Magdalena Białomazur[1), 2), *)] (ORCHID ID: 0000-0002-1093-2624), **Izabella Jasińska**[1)], **Krzysztof Kowalczyk**[2)] (0000-0003-0435-612x), **Marlena Musik**[2)] (0000-0001-5521-2893), **Kamil Pasierbiewicz**[3)] (0000-0003-4364-7363), **Rafał J. Wróbel**[2)] (0000-0003-2593-0813)

DOI: dx.doi.org/10.14314/polimery.2021.10.1

Abstract: In this work, weathering performance and durability of a commercial automotive acrylic polyurethane topcoat samples exposed at a natural testing station in an industrial atmosphere (Police, Poland) were studied. After a 16-month outdoor aging process, surface morphology and general appearance of the clearcoat were investigated by means of optical and scanning electron microscopes, an optical profilometer and by a glossmeter. For further investigation of the samples surfaces chemistry X-ray photo-electron spectroscopy (XPS) and Fourier transform infrared spectroscopy (FTIR) were utilized. Test results showed that the outdoor exposure changed the appearance of the acrylic polyurethane topcoat surface because protuberant spots of various sizes were observed. Quantitative profilometric analysis indicated an apparent increase of surfaces roughness, however, no signs of chemical degradation of the studied topcoat were revealed by XPS and FTIR analyses. Finally, it was apparent that the surface protuberances observed after the ageing test resulted by atmospheric deposits consisting mainly of oxygen, calcium, phosphorus, iron, and silicon compounds and elemental carbon. Additionally, it was revealed that a detailed cleaning process of the clearcoat surfaces may remove the detected contaminants.

Keywords: automotive coating, acrylic polyurethane coating, industrial area, outdoor weathering, FTIR, XPS.

Trwałość akrylowych powłok poliuretanowych w warunkach atmosferycznych na zewnątrz w obszarze przemysłowym

Streszczenie: W niniejszej pracy zbadano trwałość próbek komercyjnej akrylowo-poliuretanowej nawierzchniowej powłoki samochodowej w trakcie ich ekspozycji w atmosferze przemysłowej zakładów chemicznych (Police, Polska). Morfologię powierzchni i ogólny wygląd powłok lakierowych (po 16 miesiącach testu) zbadano za pomocą mikroskopu optycznego i skaningowego mikroskopu elektronowego, profilometru optycznego oraz połyskomierza. Do badań składu i struktury chemicznej powierzchni wymalowań wykorzystano rentgenowską spektroskopię fotoelektronów (XPS) oraz spektroskopię w podczerwieni z transformacją Fouriera (FTIR). Ekspozycja w atmosferze przemysłowej zmieniła wygląd powierzchni powłok gdyż zaobserwowano wypukłe plamy o różnej wielkości. Dodatkowo, ilościo-

[1)] Grupa Azoty Zakłady Chemiczne „Police" S.A., ul. Kuźnicka 1, 72-010 Police, Poland.

[2)] West Pomeranian University of Technology in Szczecin, Faculty of Chemical Technology and Engineering, Al. Piastów 42, 71-065 Szczecin, Poland.

[3)] Centrum Badawczo – Rozwojowe Partnerstwa Wschodniego Sp. z o. o., ul. Projektowa 4, 20-209 Lublin, Poland.

[*)] Author for correspondence: magdalena.bialomazur@grupaazoty.com

wa analiza profilometryczna wykazała wyraźny wzrost chropowatości powierzchni, chociaż wyniki badań metodami XPS i FTIR nie wykazały żadnych oznak chemicznej degradacji testowanych próbek. Ostatecznie okazało się, że wypukłości obserwowane na powierzchniach starzonych powłok były osadami atmosferycznymi składającymi się głównie ze związków tlenu, wapnia, fosforu, żelaza, krzemu oraz węgla. Dodatkowo wykazano, że dokładne umycie powierzchni powłok powoduje usunięcie wspomnianych zanieczyszczeń.

Słowa kluczowe: powłoka samochodowa, akrylowa powłoka poliuretanowa, obszar przemysłowy, test starzenia na zewnątrz, FTIR, XPS.

Automotive industry is one of the primary users of acrylic coatings, which are known for their aesthetic appearance, long-term weathering durability, good chemical, and mechanical resistance [1–3].

Outdoor durability of multilayer automotive coating systems depends mainly on properties of their outermost layers known as topcoats. Today, clear topcoats ("klars") based on 2K acrylic polyurethane compositions are dominant technology in Original Equipment Manufacturer (OEM) and refinish automotive coatings in Europe and they are also widely used globally [4-5]. These clearcoats with urethane cross links (resulting from a reaction of OH groups of an acrylic polyol with polyisocyanate) offer improved resistance against UV light degradation and environmental effects.

Nonetheless, acrylic clear topcoats as other protective coatings may degrade over time and lose their functional properties as a result of exposure to environmentally destructive factors such as UV, temperature, oxygen, humidity, road salt, air pollutants, microorganisms and wide range of other natural agents including bird droppings, tree gums and even dragonfly eggs [2, 6–14].

In order to evaluate coating quality and service lifetime accelerated laboratory tests and outdoor exposure in natural weathering conditions are performed. Many different accelerated tests like QUV weathering, thermal cycling, aging in cabinets with salt spray, humidity or SO_2 atmospheres and acid etching tests are commonly used to simulate various environmental influences [3, 8, 15–17].

Despite many efforts made on improvement of conventional accelerated tests such as climate alternating tests or simulation of acid rain, the problem of getting of acceptable correlation between laboratory and outdoor exposures still exists. Therefore, natural exposure in various locations (different climate and pollution level) combined with analytical techniques for early detection of chemical changes in coating materials are considered as the most reliable method for evaluating the weathering behavior of exterior coatings. However, long exposure times (minimum one year) are required in order to obtain representational data due to changes of meteorological conditions throughout the year [18].

Although outdoor weathering aging of automotive acrylic coatings are carried out in many various locations including sites with humid and warm conditions (*e.g.* Florida, south coast of France), dry and hot conditions (*e.g.* Arizona, Australia) [3, 8, 19–20] and urban environments (*e.g.* Radom, Poland) [7, 21], natural exposure tests in industrial areas are still limited; thus, there is a lack of information about durability and degradation behavior of acrylic polyurethane coatings in atmospheres commonly considered as harsh environments.

In this work, the aging behaviour of automotive commercial coating systems exposed to specific industrial environment was studied. Changes in surface topography and morphology of an acrylic polyurethane topcoat layers and their general appearance were monitored by optical and scanning electron microscopes, an optical profilometer and by a gloss reflectometer. The alternations of chemical structure after exposure were analysed by two complementary techniques: X-ray photoelectron spectroscopy (XPS) and Fourier transform infrared spectroscopy (FTIR). Special emphasis was given to distinguish between surface contamination and possible destruction of the tested acrylic polyurethane clear topcoat.

EXPERIMENTAL PART

Sample preparation

The automotive industrial three-layer coating system (i.e. primer, basecoat, and clear topcoat; Spectral Coating Technology, Novol, Poland) was applied by an air spray wet-on-wet technique on blast cleaned steel panels (76 × 152 × 0.8 mm) in a professional car paint workshop. The samples were prepared in two versions using silver and black color basecoat compositions. Specific chemical composition of the topcoat is unknown, however, it is based on a hydroxyacrylic copolymer and an isocyanate hardener (HDI, hexamethylene diisocyanate). Thicknesses of the dry coating were 65±10 μm (after conditioning at room temperature for 21 days). Before their outdoor exposure, the edge of the coated panels were protected using an anticorrosive vinyl paint.

Outdoor weathering exposure

Outdoor exposure test was performed according to internal factory standards for 16 months (from May 2019 to September 2020) at an industrial area near fertilizer and inorganic chemicals plants of the Grupa Azoty

Zakłady Chemiczne "Police" S.A. company in Police, which is a town in the northern Poland. A natural testing station with weathering racks met the requirements of the PN-EN ISO 2810:2005 standard. Each color version of the coating system had five replicates. The samples were exposed with 45° tilt angle, facing south. During the weathering test, changes of specular gloss were monitored according to a planned measurement programme (with decreasing frequency). The air temperature and relative humidity were also measured and registered.

After the field exposure, all the samples were cleaned with a soft solution of car shampoo and stored in the dark place under office condition. Next, two replicates of each color version were also cleaned according car detailing procedure, which was similar to cleaning methods commonly used in commercial car washes. The three-step cleaning program consisted of pre-cleaning, a decontamination process (*i.e.* chemical removal of all kinds of tightly bonded deposits and dirt from the surface of a vehicle) with commercial detergents and dirt removing using a smooth automotive clay bar.

The surface characteristic of the automotive coating were investigated using optical profilometry, optical microscopy, scanning electron microscopy (SEM), Fourier transform infrared spectroscopy with attenuated total reflectance (FTIR-ATR) and X-ray photoelectron spectroscopy (XPS). Prior to the SEM, FTIR and XPS measurements the coating samples were cut into round specimens with a diameter of 1 cm.

Characterisation methods

Infrared spectroscopy

FTIR-ATR spectra of the automotive clear topcoat samples were obtained using the Thermo Fisher Scientific Nicolet FTIR 380 spectrometer (Waltham, MA, USA) equipped with an ATR diamond plate. Spectra were recorded in the transmittance mode from 400 to 4000 cm^{-1}, with a resolution of 4 cm^{-1}.

XPS measurements

The X-ray photoelectron spectroscopy measurements were carried out in a commercial multipurpose (XPS, LEED, UPS, AES) UHV surface analysis system (PREVAC), which operates at a base pressure in the low 10^{-10} mbar range. The calibration of the X-ray photoelectron spectrometer was performed using Ag 3d5/2 transition. An analyser chamber was degasified prior to measurement so that during XPS measurements the pressure was in the low 10^{-9} mbar range. The X-ray photoelectron spectroscopy was performed using K_α of aluminum (h = 1486.6 eV) radiation. Due to charging effects, the binding energy scale was calibrated using C1s (aliphatic carbon bonded to another carbon) transition at 285.0 eV. The C1s and N1s regions were deconvoluted using the CasaXPS software (V2.3.15 CASA Software Ltd., UK).

Optical profilometry measurements

The samples were analysed using the Contour GT optical profilometer (Bruker, USA). Basic surface roughness parameters and their 3 D surface topography maps were obtained. Three repetitive measurements were made on each sample with the analysed area of 4 mm^2.

Microscopic analysis

Optical microscopic images of the coating samples were recorded by means of the Stemi 508 optical microscope (Carl Zeiss, Germany). Morphology characteristic of the samples was observed using the SU8020 scanning electron microscope (Hitachi, Japan) with the accelerating voltage of 5 kV. In order to avoid charging effects, the specimens were coated with 10 nm chromium layers prior to the SEM imaging. A coater (Q150T ES; Quorum, UK) equipped with a turbomolecular pump was used.

Specular gloss measurements

Surface specular gloss was measured using the Haze-Gloss reflectometer at a 20° incidence angle (BYK-Gardner, Germany). The presented data were averaged using results of three measurements of a single panel; the measured area was a circle with a diameter of 15 mm. Gloss retention of the coatings was expressed as a percentage of the initial gloss value.

PM10 samples chemical characterisation

Four PM10 particulate samples were collected on quartz fibber filters (QMA 1851 047; Whatman, UK) in November 2018 at the environmental monitoring station belonging to the chemical plant in Police (located ca. 0.5 km of the natural testing station). All the samples were analysed for ionic components concentration (Cl^-, NO_3^-, PO_4^{3-}, SO_4^{2-}, NH_4^+, K^+) by ion chromatography (Dionex ICS 1100, Thermo Scientific, UK). The thermo-optic analyzer (Model-4L, Sunset, USA) with flame ionization detection (FID) was used to determine organic (OC) and elemental carbon (EC).

RESULTS AND DISCUSSION

Outdoor weathering data

According to meteorological data presented in the previous work [22], the climatic conditions in the coated samples exposure location (Police) are typical for the north-western part of Poland, with annual average temperature of 9.4°C, relative humidity of 80.3%, and 563.6 mm of total rain per year. Due to the warm and

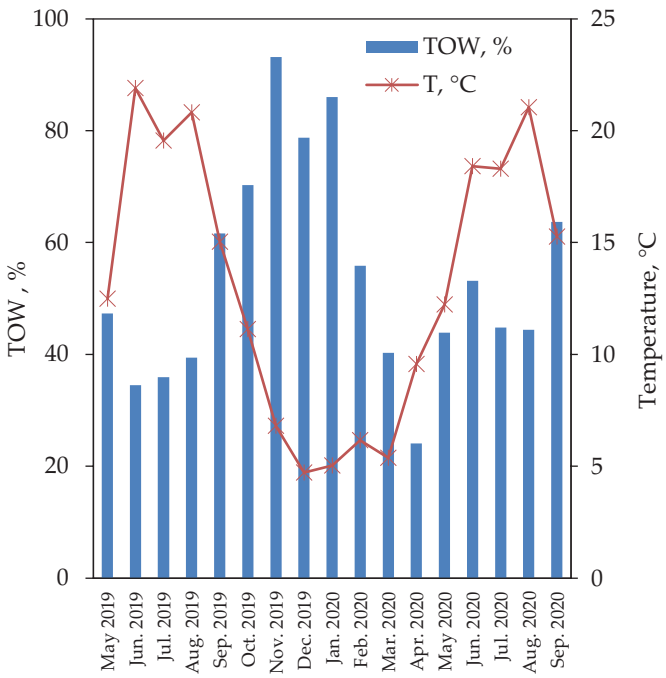

Fig. 1. Average temperature and %TOW for Police from May 2019 to September 2020

fully humid climate determined for this part of Poland [23], the time with high humidity was considered as the important environmental factor, which may be responsible for organic coating degradation processes. The time of wetness (TOW) – defined as the fraction of time in which the relative humidity is higher than 80% and the temperature is higher than 0°C (ISO 9223, 2012) – was determined on the basis of meteorological data registered during the test period. Monthly changes of average temperature and TOW expressed as the percentage of wet conditions are presented in Fig. 1. The seasonal oscillations of these parameters were observed, especially with low average temperature and very long time of wetness during the autumn and winter. The TOW calculated for total exposure time was 53.9%, which means that samples exposed in natural testing station were stored in high humidity conditions for 6709 hours. During that wet periods water condensation on the coating surface and high water uptake may occur [15] and led to deterioration of coating features [2].

Surface topography and morphology evaluation

Optical as well as scanning electron microscopy techniques were utilized to investigate the surface morphology of the tested topcoat with respect to outdoor weathering performance. In addition, basic surface roughness parameters and 3D microscopic views were obtained.

Figure 2 shows optical micrographs (55×) of silver and black color coatings before their exposition (the reference samples) and after exposure in outdoor conditions in the industrial area for 16 months (without and with further cleaning according to a special car detailing procedure). The micrograph of the unexposed silver color sample revealed aluminum flakes with grainy appearance, that visually provide a texture [3]. In case of unaged black color coating the bright sparkles over a darker background were observed (probably metallic pearls in the basecoat). However, both silver and black color reference coatings were relatively homogenous with regular patterns. After the 16-month outdoor exposure, some morphology differences were found on the aged surfaces. The presence of some small, circular, dark spots on silver color sample and the appearance of widespread white stains on black surface, may be related to the fact that dark features are easier to be observed on bright colors and vice versa [9]. Nevertheless, the nature of these different surface features cannot be clearly assessed. Coatings during outdoor weathering can deteriorate over time as a result of exposure to many different environmental factors such as UV, heat, sand abrasion, humidity, chemical and biological attack [2]. Color change, gloss reduction, cracking, blistering and other deformities can then occurred [3]. The results of natural weathering tests may be also affected by the contamination of the coating after the exposure [24]. Therefore, the regions that appear to be degraded can simply contain impurities in form of deposit. Although all the samples were cleaned with soft solution of car shampoo after the field exposure, the observed changes could still be considered after washing as the remains of the deposited material. It was regarded as possible, especially in case of white stains on black color samples which were visible to the naked eye. To investigate the nature of stains on coating surfaces (after the outdoor exposure), the attempt to remove them was done. Aiming that, two replicates of each color system were additionally cleaned according to a car detailing procedure commonly used in commercial car washes in order to removing tightly bonded contaminants such as airborne compounds, tree saps, industrial fallouts, rail dust and plain road grimes. As could be observed in Fig. 2 (c and f), the coating surfaces after superior cleaning performance appear to be similar to that of the unexposed samples. The slight scratches registered on the detailed cleaned black color coating were most likely created during the sample preparation for the surface investigations.

Similar results were registered by means of the SEM technique, especially at higher magnification (Fig. 3). After the outdoor exposure, some features with pronounced structures appeared on the surfaces of both silver and black color samples, but no evident damages were observed on the detailed cleaned panels.

The 3D topographic images, obtained using the optical profilometer, show that surfaces of aged coated samples (Figs. 4b and 4e) became rough and obvious small spikes and larger protuberances of various sizes appeared. Quantitative profilometric analysis indicated an evident increment of the roughness.

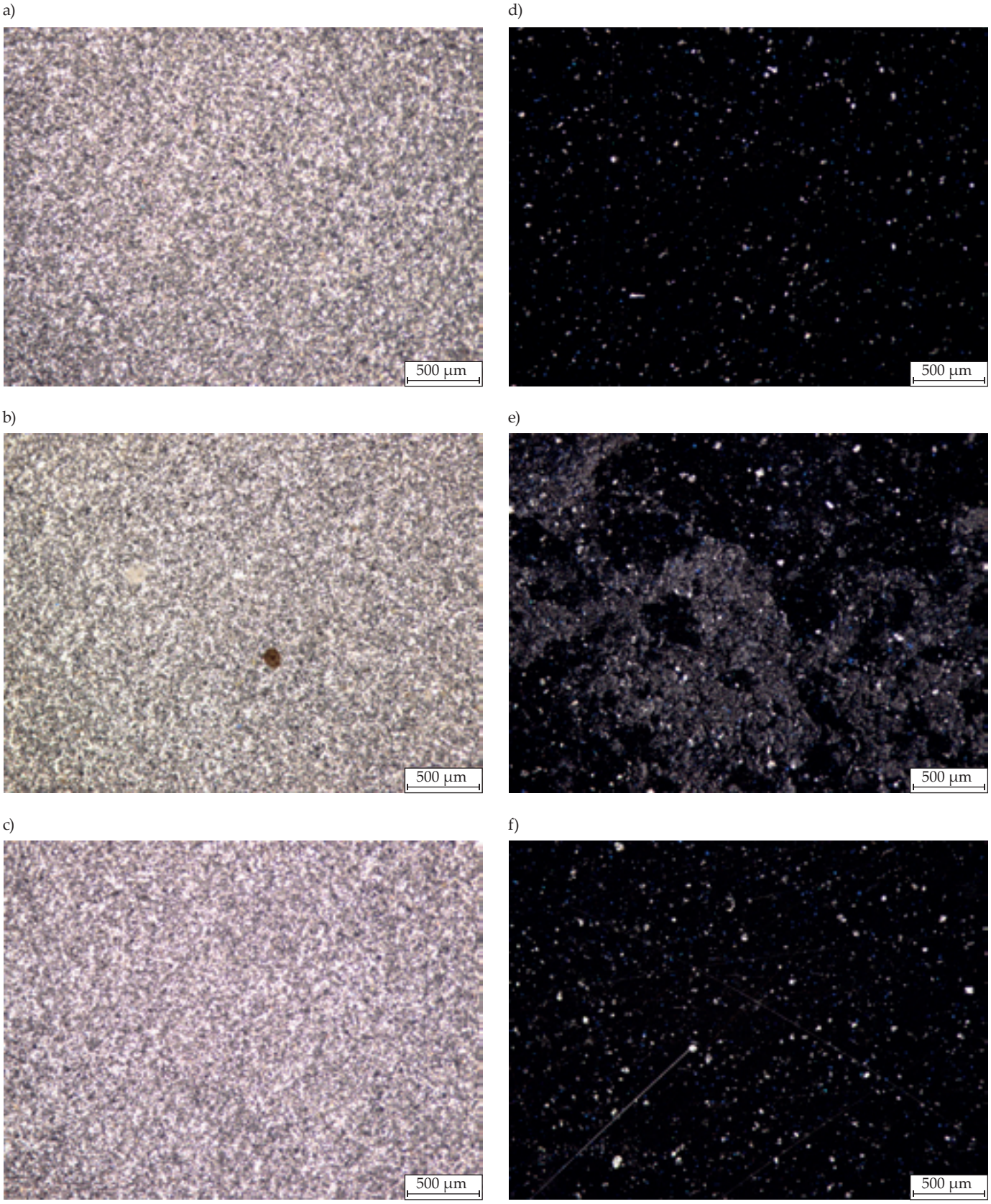

Fig. 2. Optical micrographs of the: a) unexposed silver color coating, b) exposed silver color coating, c) exposed and cleaned silver color coating, d) unexposed black color coating, e) exposed black color coating, f) exposed and cleaned black color coating

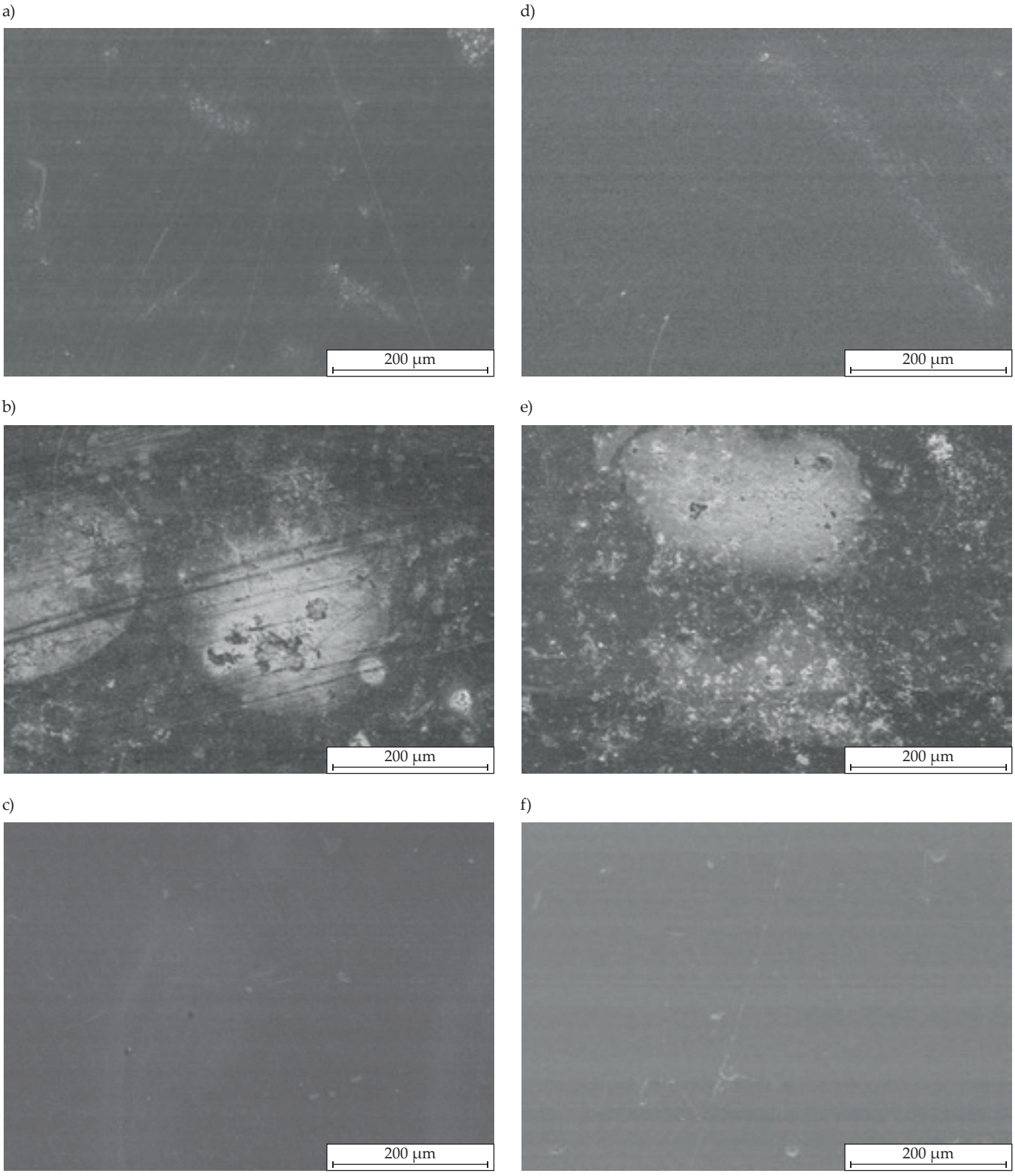

Fig. 3. SEM images of the: a) unexposed silver color coating, b) exposed silver color coating, c) exposed and cleaned silver color coating, d) unexposed black color coating, e) exposed black color coating, f) exposed and cleaned black color coating

T a b l e 1. Surface roughness parameters from representative regions of the silver and black color coatings

Sample	R_a, µm	R_q, µm
Silver, unexposed	0.225	0.277
Silver, exposed	0.653	2.141
Silver, exposed and cleaned	0.162	0.355
Black, unexposed	0.134	0.199
Black, exposed	0.580	0.987
Black, exposed and cleaned	0.186	0.254

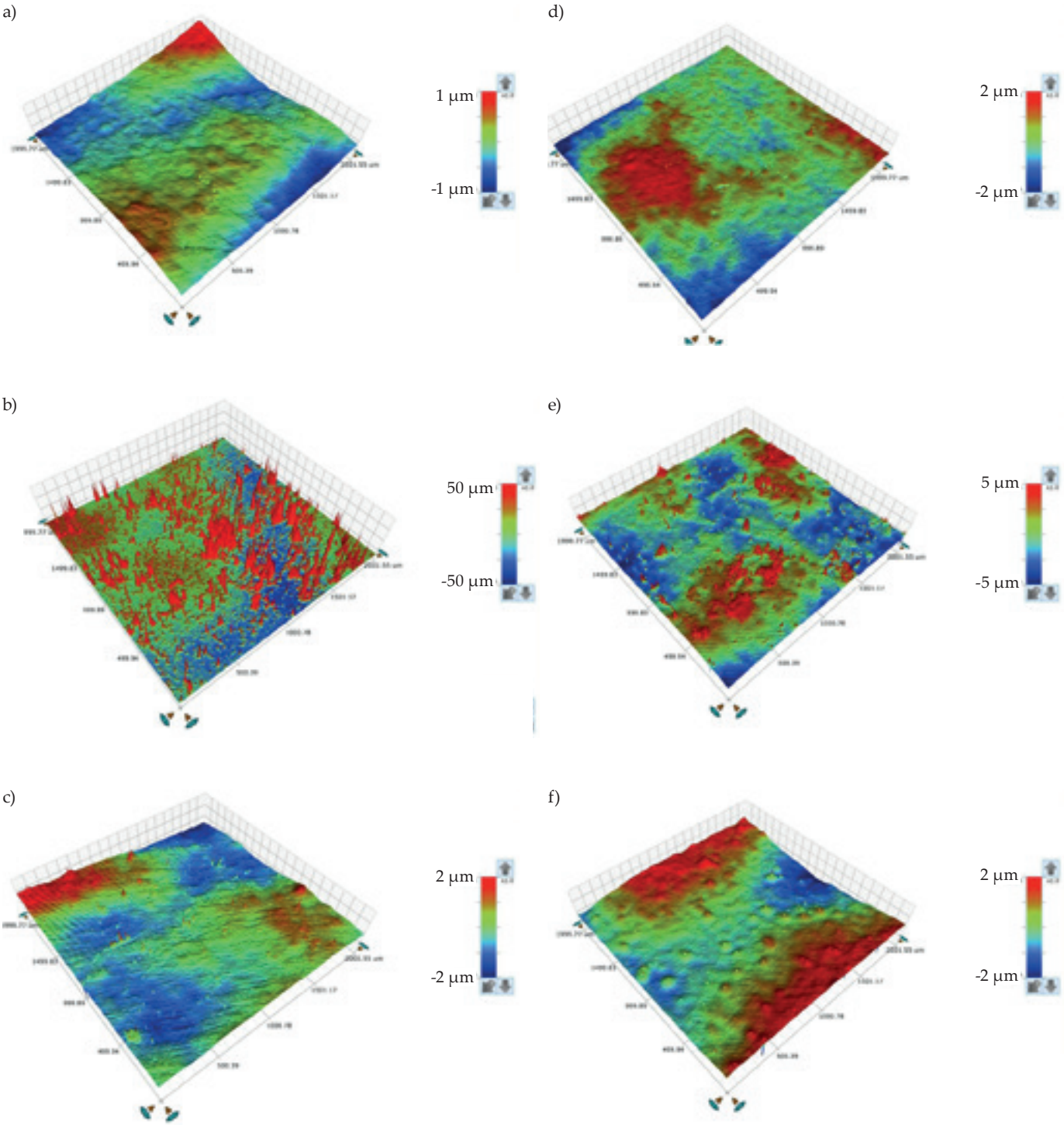

Fig. 4. 3D microscopic views of sample surfaces of the: a) unexposed silver color coating, b) exposed silver color coating, c) exposed and cleaned silver color coating, d) unexposed black color coating, e) exposed black color coating, f) exposed and cleaned black color coating

According to the Table 1, the average roughness (R_a) and root-mean square roughness (R_q) of the field exposed samples reached the values of three or even four times greater than the parameter noted for the reference panels. Both widespread low protuberances and depressions were found on the clearcoats of the detailed cleaned silver and black color panels. However, the height or depth of those surface unevenness was 2 μm or less and the Ra and Rq values were similar to those measured for the reference samples. It can be summarized that the surface topography of the reference samples - but also of the exposed and detailed cleaned samples - was relatively similar and flat.

Gloss retention

To study the effect of outdoor weathering on general appearance and optical quality of the coating surface, specular gloss was measured during the field exposure. Variations of the gloss retention, i.e. the parameter calculated as a percentage of the initial gloss that retained after the exposure, for the silver and black color samples before and after the additional detailed cleaning is presented in Fig. 5.

The recorded values for all the panels did not reveal relevant changes; both color-type samples exhibited the high gloss retention values after the 16-month exposure (> 92%) and they were increased to the initial values by the additional cleaning process. This indicates high resistance of the acrylic polyurethane clear topcoat to environmental influences and a slight effect of the weathering conditions on the aesthetic properties of the tested coating materials [10]. Comparable small reduction of surface gloss of acrylic polyurethane coatings was observed during a 20-month natural exposure test performed in Ha Long city in Vietnam [25]. The gloss retention results are also consistent with small changes of surface roughness values measured during our natural weathering tests. It is not unexpected, because loss of gloss is most often correlated with an increment of surface rugosity [19].

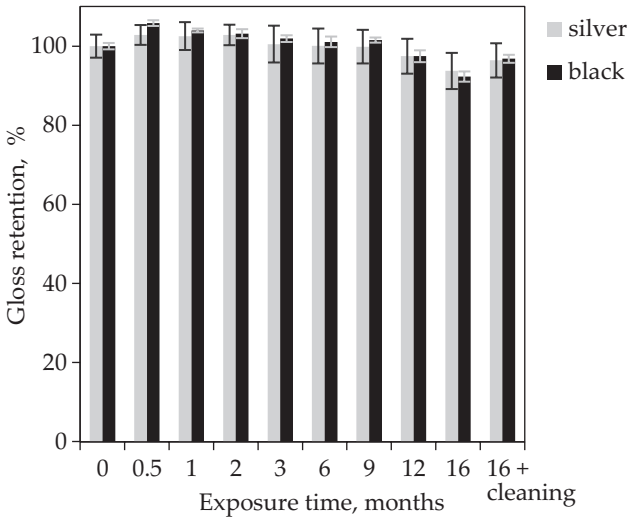

Fig. 5. Retention of gloss (20°) in relation to the outdoor exposure time

XPS results

The XPS (X-ray photoelectron spectroscopy) is a widely used technique for surface chemical analysis of polymer coatings [26-27]. In recent years, an increment of this method application to evaluate degradation of various organic coatings has been observed [28-30]. Due to advantages of the XPS method related to its high surface sensitivity and possibility of chemically specific identification of carbon [26, 31] , we considered this technique as an useful tool to characterize the surface of the clear acrylic polyurethane topcoats during the natural weathering test; the XPS studies were performed in order to characterize the changes of coating surface chemistry after 16-month outdoor exposure. XPS spectra of the three silver color coatings, i.e. the reference, exposed as well as exposed and detailed cleaned samples, are present in Fig. 6.

The carbon (at 285 eV), oxygen (at 535 eV) and nitrogen (at 400 eV) were found dominant in surface composition of unexposed sample. Nitrogen is especially characteristic for urethane links created by isocyanates in crosslinked acrylic polyurethane coatings. The other detected elements (Si, Al, Mg, and S) are suspected to be introduced to the clearcoat composition by specific auxiliary additives (*e.g.* defoamers, leveling agents) [32]. Nevertheless, their atomic contents did not exceed 1% (Table 2).

As can be seen in Table 2, atomic content of C and O elements changed remarkably after the coating exposure to outdoor weathering (no cleaning); additionally, two new elements (P and Fe) were detected on the surface of both silver and black color coatings. A slight but evident increment of Si, Al, and Ca concentration was also observed. Generally, the oxygen/carbon (O/C) ratio after the field exposure doubles (Table 3).

T a b l e 2. Elemental composition of the coating surfaces

Coating treatment	Atomic percentage, %									
	C	N	O	S	Ca	Al	Si	Mg	P	Fe
Silver, unexposed	76.8	3.4	17.1	0.1	0.2	0.6	0.8	1.0	-	-
Silver, exposed	64.3	2.8	26.7	0.2	0.4	1.0	2.7	0.5	1.0	0.4
Silver, exposed and cleaned	80.1	2.4	14.7	0.2	0.3	0.2	0.8	1.2	-	-
Black, unexposed	80.6	2.9	14.7	<0.1	0.1	-	0.6	1.1	-	-
Black, exposed	57.9	3.5	31.7	-	0.7	1.0	2.5	0.4	1.8	0.5
Black, exposed and cleaned	77.4	3.3	17.3	0.1	0.1	0.1	0.2	1.5	-	-

T a b l e 3. Atomic ratios for the coating surfaces

Coating treatment	Atomic ratio	
	N/C	O/C
Silver, unexposed	0.04	0.22
Silver, exposed	0.04	0.42
Silver, exposed and cleaned	0.03	0.18
Black, unexposed	0.04	0.18
Black, exposed	0.06	0.55
Black, exposed and cleaned	0.04	0.22

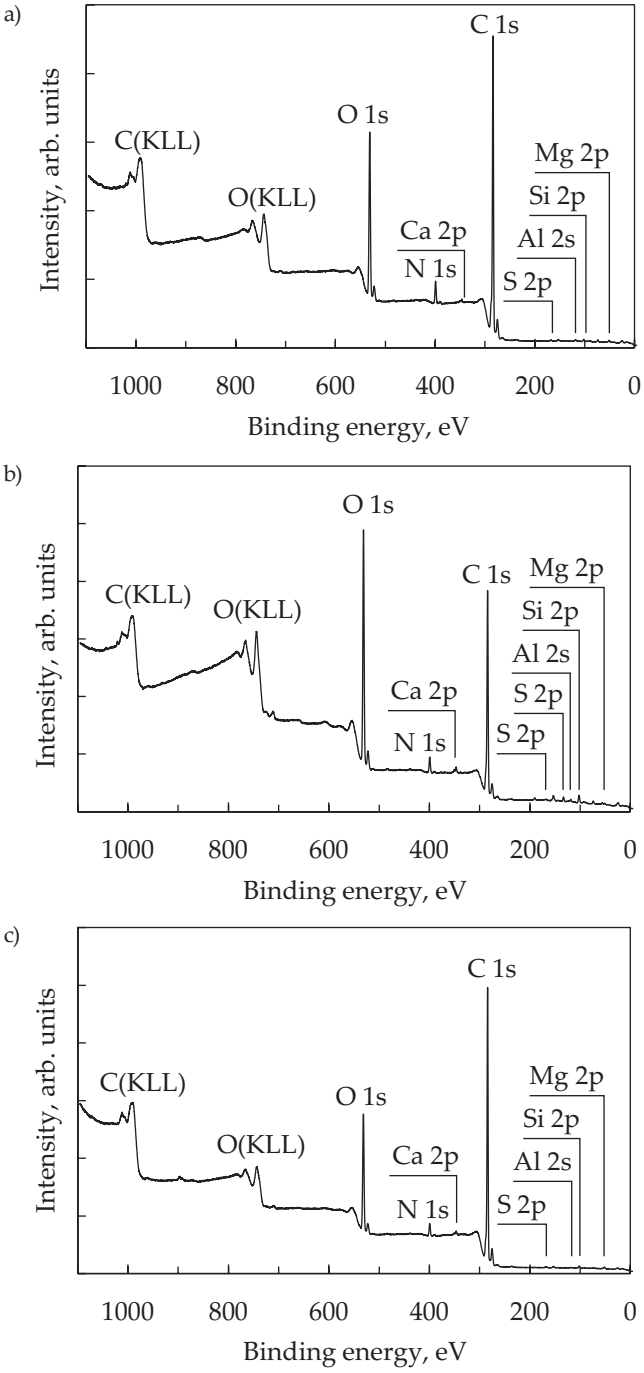

Fig. 6. XPS full spectrum of the silver color samples: a) unexposed, b) exposed, c) exposed and cleaned

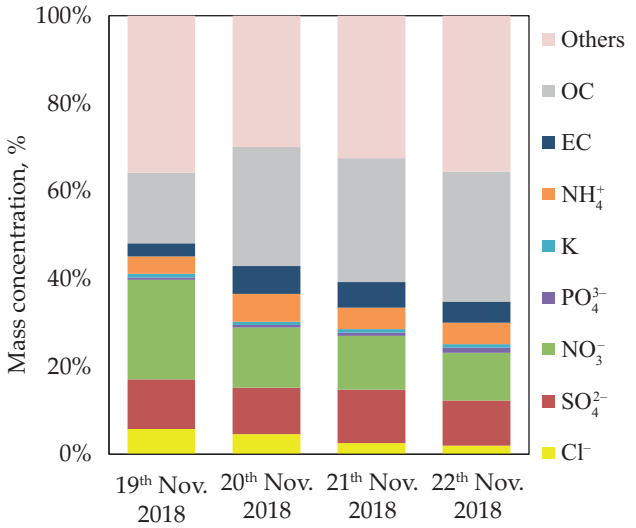

Fig. 7. Percentage of particular compounds in PM10 samples collected in the area of the natural testing station

This growth could be related to degradation/oxidation of the polymer matrix [28-29, 33]. However, in this study, another explanation should be considered as well. Perhaps the O/C increment results from the deposits presence on the coating surface containing insoluble oxygen-rich minerals, especially since XPS analysis provides information on a near surface region, i.e. in the range of 1 – 10 nm [34]. It can be also confirmed by slight increase of the Si, Al and Ca elements content on the aged surfaces and by the presence of P and Fe elements (the characteristic components of air contaminants in the Police fertilizer factory). On the other hand, the XPS data shown no significant changes of the nitrogen/carbon ratio (N/C; Table 3), because the N-based component (NH_4^+) were also detected in the air contaminants (Fig. 7).

Finally, the elemental analysis results for the panels (after their additional detailed cleaning) were quite similar to those observed for the reference samples – it suggests that ester and polyurethane linkages in crosslinked acrylic resins still remain intact.

In the case of no significant changes of chemical composition of the coatings surfaces, the high-resolution XPS spectra of C1s were deconvoluted for each analyzed sample; the obtained signals and their deconvolution are shown in Fig. 8.

Information on XPS studies of automotive acrylic clearcoats has not been found anywhere in a literature. Therefore, the deconvolution of the C1s spectrum for the reference samples was performed based on the data reported for polyacrylic acid (PAA) [35] and poly (methyl methacrylate) (PMMA) [36], where the high-resolution C 1s spectra were resolved into four characteristic peaks. In addition, a set of constrains was applied in order to ensure adequate interpretation of changes caused by outdoor weathering process of the coatings. Once the spectra for the reference sample were curve fitted, the FWHM (full width at half maximum) and position in BE were constrained, and then applied to the XPS curves determined

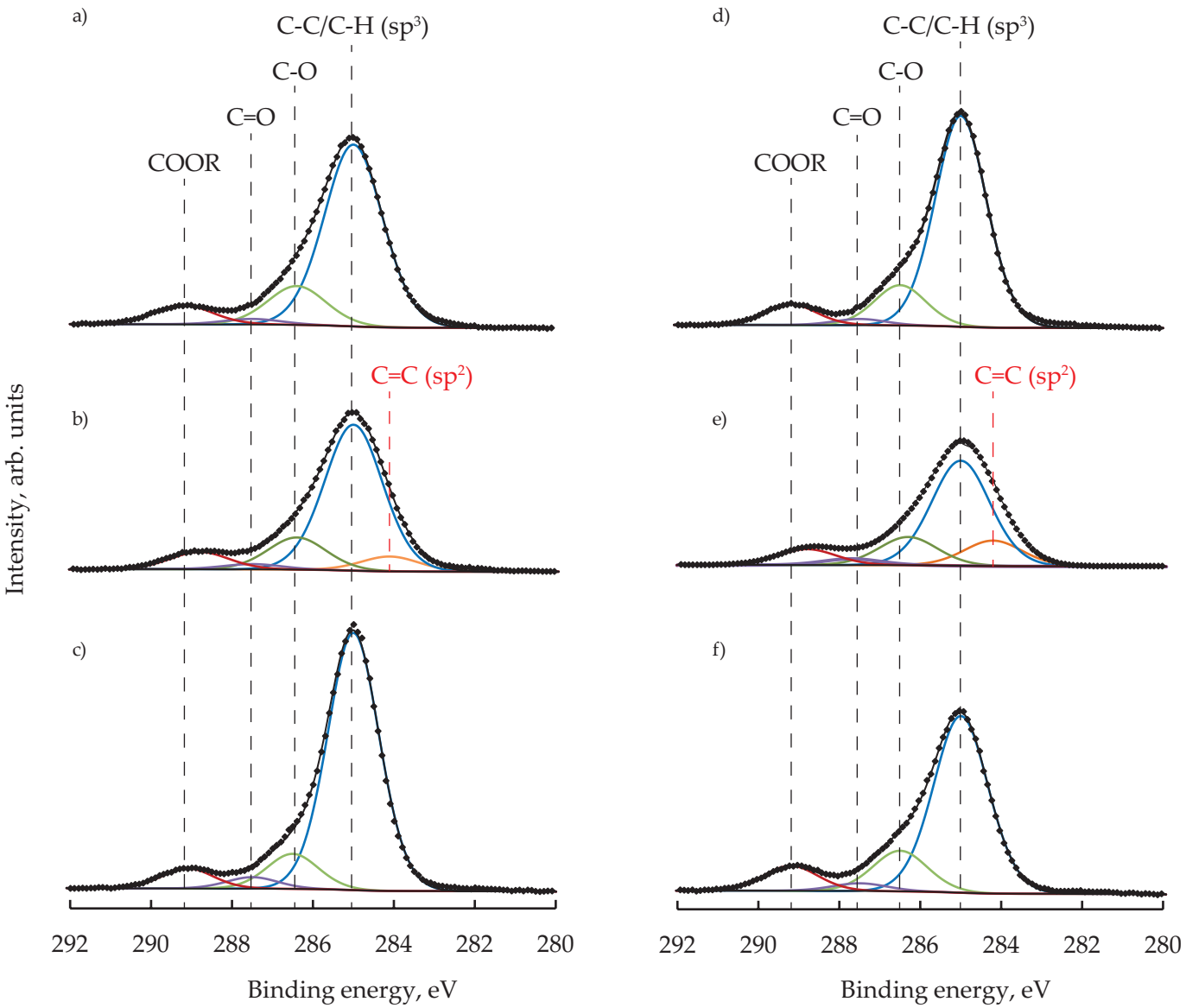

Fig. 8. The deconvoluted C1s XPS spectra for the: a) unexposed silver color coating, b) exposed silver color coating, c) exposed and cleaned silver color coating, d) unexposed black color coating, e) exposed black color coating, f) exposed and cleaned black color coating

for other samples in studied series. The peaks were fitted with FWHM of 1.5 – 1.7 eV (with the additional assumption that all peaks within one deconvoluted curve had the same value) and the binding energies were: C-C/C-H 285.0 ± 0.2 eV, C-O 286.5 ± 0.2 eV, C=O 287.5 ± 0.2 eV and COOR 289.0 ± 0.2 eV. These positions are consistent with those reported for polymer samples by Briggs and Seah [37].

The absence of the peak for C-N bonding can be explained by a very low content of nitrogen measured during XPS full spectrum analysis. It indicates much lower C-N bonding distribution compared to C-C and C-O bonding [26]. It is also noteworthy that satellites were not included in our curve-fitting procedure, because their intensities were practically invisible and had no influence on the obtained results.

As shown in Figs. 8 b and 8 f, after the outdoor exposure of the acrylic polyurethane coatings no significant changes were recorded for left peak shoulder related to formation of carbon oxygen bonds. Interestingly, more pronounced change is visible in right shoulder that is less steep. In addition to the polymer peaks, the one at 284.1± 0.2 eV appeared for both silver and black color coatings. The new peak is lying lower in energy by about 0.9 ± 0.2 eV then the component attributed to the functional groups of C-C/C-H. According to the literature, the lower energy component with shift of 1.1 ± 0.2 eV towards lower binding energies in relation to peak C-H (sp^3), is associated to sp^2-bonded carbon atoms [38]. The presence of the peak at 284.2±0.1 eV was reported to be found in the XPS high-resolution C1s spectra of the atmospheric particulate matter PM collected in urban and industrial areas [39–40]. This low binding energy component was assigned by the authors of these works to elemental carbon. Similar observation were noted for road dusts

T a b l e 4. The content of C1s components expressed as molar fractions

Assignment	Silver coating			Black coating		
	Unexposed	Exposed	Exposed and cleaned	Unexposed	Exposed	Exposed and cleaned
sp^3 C-C/C-H	0.74	0.68	0.79	0.76	0.58	0.71
sp^2 C=C/C-C	–	0.07	–	–	0.14	–
C-O	0.16	0.15	0.11	0.15	0.16	0.16
C=O	0.02	0.02	0.04	0.02	0.03	0.03
COOR	0.08	0.08	0.06	0.07	0.09	0.10

sampled near coal power plant, where the peak, corresponding to the formation of C=C bonding, was recorded at 284.3–284.6 eV [41]. That phenomenon - and the fact that organic and elemental carbon constituted a remarkable proportion of the total PM10 samples collected in the area of the natural testing station (Fig. 7) – indicates that the 284.1± 0.2 eV signal originates form carbon species adsorbed on the surface of the coating panels during their outdoor exposure. Moreover, the detailed cleaning of the exposed panels resulted in the C1s spectra similar to those recorded for the reference samples (i.e. without additional peak for C=C bonding).

The results of quantitative analyses of deconvolution of C1s signals (presented in Fig. 8) are listed in Table 4.

Apart from the appearance of a new peak assigned to carbon originating from surface deposits and a proportional decrement of the C-C/C-H groups content, there are no significant differences in the atomic concentration of the C1s groups. The slight changes observed for the forms of oxidized carbon seem to be rather irrelevant, and may result from some variation of the initial chemical composition of the coating replicates.

In this work, the high-resolution XPS spectra of O1s were considered to be very complex and virtually impossible to accurately and unambiguously conduct the curve-fitting process. The broad oxygen signals ranged between 528 and 536 eV for all the coating samples. Due to high probability of multiple overlapping peaks (which can be attributed to the oxygen bonds in polymers as well as to SiO_2, sulfates, phosphates and other inorganic compounds from material deposited during outdoor exposure), interpretation of O1s spectra was not realized.

As far as the nitrogen is concerned, Fig. 9 presents N1s curves for the reference and the exposed (without the superior cleaning) silver color samples. Almost all the studied samples gave the similar N1s signals, which have been interpreted as a one component peak (at 400.0 ± 0.2 eV) originating form N-C group (in the urethane bond) present in crosslinked acrylic polyurethane coatings. One exception was for the silver color sample after the 16-month exposure, whose N1s spectrum was fitted with two different components (at 400.0 eV and 401.9 eV). The new small peak at 401.9 eV may results from appearance of quaternary nitrogen, which has been attributed to ammonium ion. It has been reported in the literature that ammonium ion XPS peaks were observed in samples of various atmospheric particulates [39, 42–43]. The presence of ammonium ions in atmospheric particles has been confirmed during bulk chemical analysis of PM10 samples collected at an environmental monitoring station belonging to the chemical plant in Police (Fig. 7). Thus, it is most probable that ammonium salts are the minor constituents in the surface depositions, which were not dissolved during rains or cleaning with the soft solution of car shampoo.

The XPS data suggest that chemical nature of the outermost clear layers of the coating system (tested for

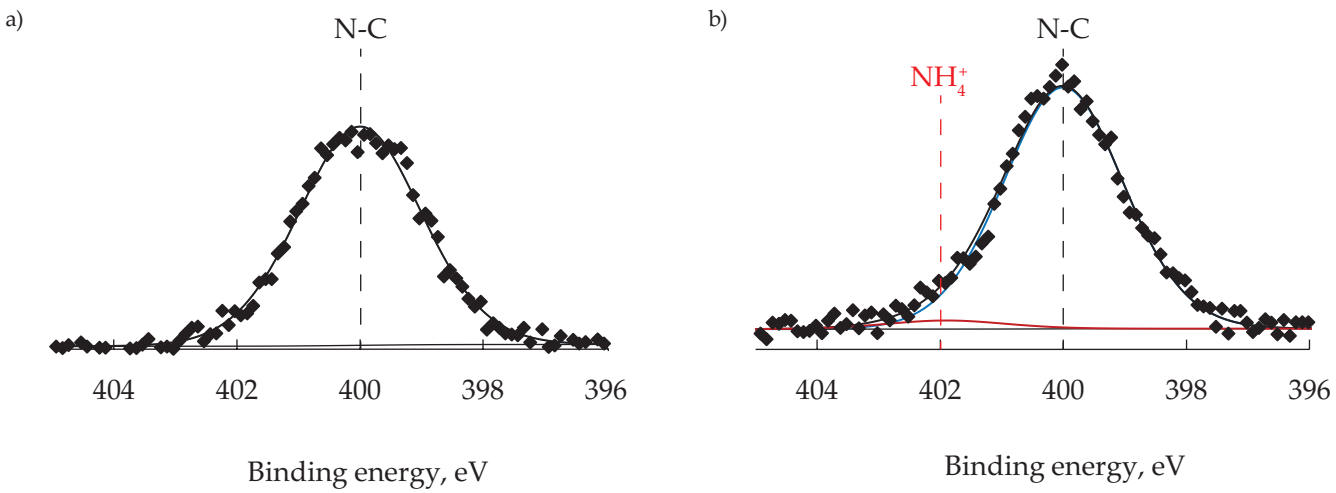

Fig. 9. The deconvoluted N1s XPS spectra for the: a) unexposed silver color coating, b) exposed silver color coating

16 months in the vicinity of chemical and fertilizer plants) remained unchanged. It is apparent that the small, circular, dark spots and widespread white stains visible on the exposed samples surfaces are atmospheric deposits containing mainly oxygen, calcium, phosphorus, iron, silicon, and elemental carbon.

FTIR results

In order to provide more comprehensive information about morphological changes of the outdoor-exposed automotive coatings, the XPS analysis was complemented with the FTIR-ATR technique allowing detection of chemical changes in an organic coatings surfaces, even at a very early exposure stage [44-45]. Due to the fact that the signal originates from 1-3 μm of material, the FTIR-ATR is acknowledged to be a surface sensitive technique suitable for automotive coatings investigation [46].

Fig. 10 shows FTIR-ATR spectra for the six panels in the silver and black color versions (i.e. the reference, exposed as well as exposed and detailed cleaned samples). All the spectra were normalized using CH_2 bending vibration (1460 cm^{-1}) due to its relatively high stability during coating properties deterioration processes [18, 47]. The assignments for main characteristic absorption bands registered for the studied acrylic polyurethane topcoat are listed in Table 5 [19, 20, 48–54].

The strong intense doublet observed at 1723 cm^{-1} and 1683 cm^{-1} is characteristic for an urethane modified acrylic clearcoat [50, 55] while the shape of IR spectra in the fingerprint region (from 1100 cm^{-1} to 1300 cm^{-1} with the highest intensity peak at 1147 cm^{-1}) represents an acrylic binder [50]. Another characteristic peak (corresponding to the coupling of N-H bending vibration with C-N stretching vibration in the HN-C(O) group (known as an amide II band)) was recorded at 1528 cm^{-1}. This one is very important in relation to weathering results since a loss of its intensity is considered as a major sign of acrylic polyurethane coating degradation due to a photo-induced scission of polyurethane cross links

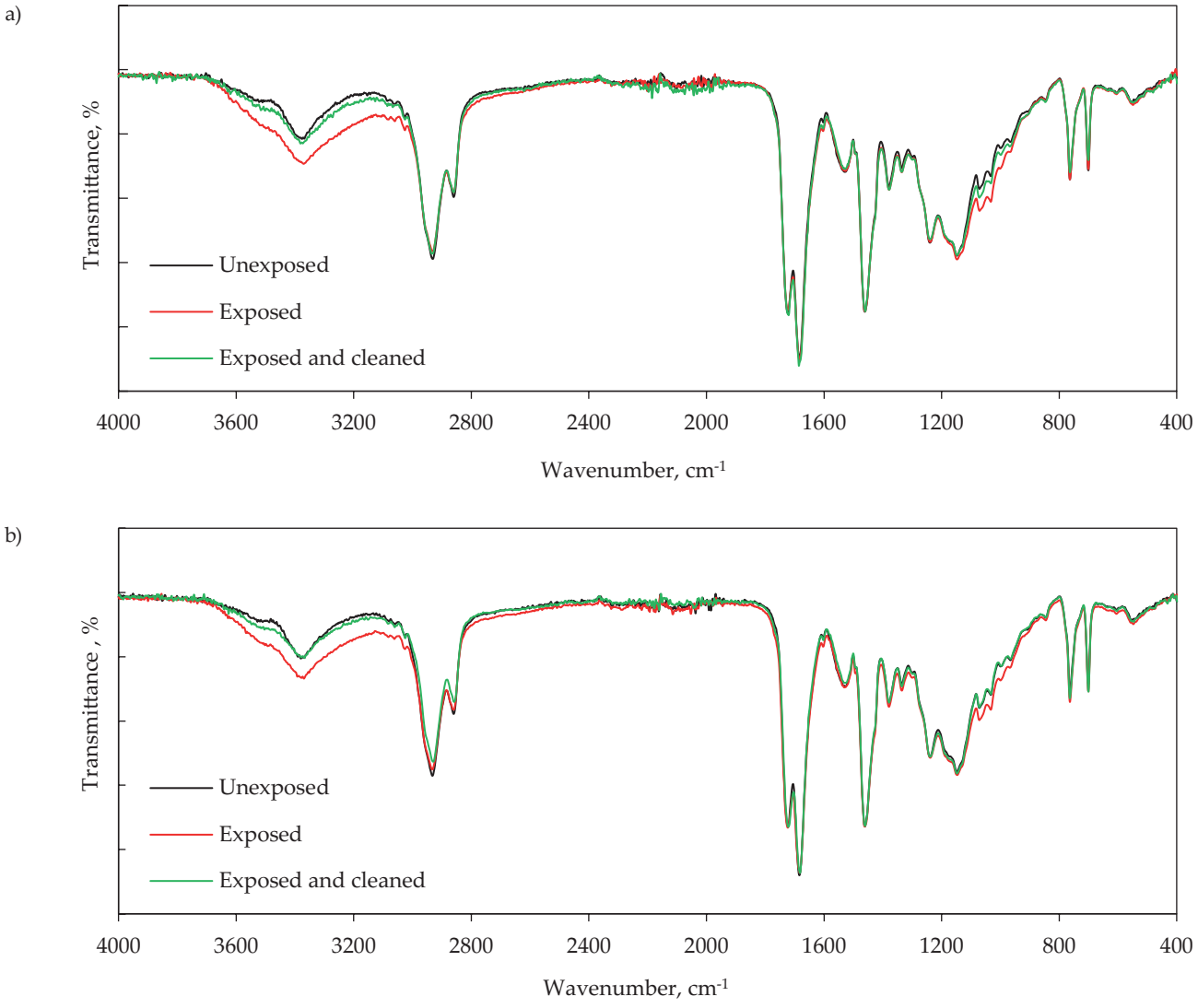

Fig. 10. The FTIR spectra of the: a) silver color coatings, b) black color coatings

T a b l e 5. The main FT-IR absorption bands registered for the clear topcoat of the unexposed black color coating

Frequency cm^{-1}	Main assignments	References
3379, 3450	ν(NH), ν(OH)	[20, 48, 49]
2931	$\nu_{as}(CH_2)$	[48, 49]
2859	$\nu_{sym}(CH_2)$	[48]
1723	ν (C = O) ester	[20, 48, 50, 51]
1683	ν (C = O) urethane	[48, 19]
1528	ν (C-N) + δ(N-H) (amide II)	[48, 19, 52]
1460	$\delta(CH_2)$	[48, 52]
1378	$\delta(CH_3)$	[48]
1239	ν (C − O) ester or ν (C-N) + δ(N-H) (amide III)	[48, 50, 53]
1147	ν (C − O) ester	[48, 50, 53]
763	CH (out of plane – styrene) or isocyanurate ring	[48, 50, 54]
701	= C − H (aromatic ring - styrene)	[50, 54]

[19, 51–52]. Moreover, reduction of intensity of the band at ca. 1240 cm^{-1} (C-N/N-H) [19] and notable changes in the 1600–l800 cm^{-1} region was also reported in researched literature [19, 21, 52].

Comparison of the recorded spectra for the reference and exposed samples (Fig. 10) indicates a significant intensity increment (after the outdoor exposure) of the broad band at 3100–3700 cm^{-1} (OH, NH stretching vibration), which may be caused by degradation products formation [12, 20, 25, 48, 52, 56]. The increase of the surface concentration of NH and OH groups should be correlated with cleavage of urethane bonds and creation of the amine and hydroxyl groups, however, the generally negligible changes of the IR spectra for the exposed samples vs. the reference materials (*i.e.* slightly lower peaks for HN-C(O) group at ca. 1510–1530 cm^{-1}, C=O group at ca. 1685 cm^{-1}, and C(O)-O group in the region of 1100–1300 cm^{-1}) indicate that chemical structure of the tested polymer binder was rather intact. In this case, the increment of the peak at 3100-3700 cm^{-1} should be rather assigned to the presence of water in the surface inorganic deposits. It is noteworthy that a significantly increment of a peak at the 3000-3700 cm^{-1} frequency range (registered for a polyurethane/polysiloxane hybrid coating after its ageing in marine conditions) was explained in a published paper by water absorption on a coating [48]. This interpretation is also supported by the results obtained in the present investigation for the detailed cleaned samples, whose IR spectra practically do not differ from those recorded for the reference coating panels. A slight reduction of the C-H aliphatic stretching bands intensities (at 2931 and 2859 cm^{-1}) may be assigned to initiation of polymeric chain scission due to natural photodegradation processes [20, 25, 51, 53, 56].

The small changes noticed for the 980-1150 cm^{-1} frequency range (after the field exposure) may be attributed to the presence of various inorganic species in the surface deposits, e.g. SO_4^{2-} (IR bands around 1080–1150 cm^{-1}) [57-59], PO_4^{3-} (1000 – 1100 cm^{-1}) [57, 60], and silicon compounds (ca. 1030 cm^{-1}) [58, 61-63].

Taking into consideration that all the noteworthy variations observed in IR spectra were attributed to the presence of water or other inorganic surface contaminations as well as the XPS data analysis and the visual evaluation indicated only a presence of surface contamination after outdoor exposure, it can be claimed that the chemical structure of the clear topcoat was not modified during the test in the industrial conditions. The problem of potential dirt contamination of clearcoat samples during their natural weathering was mentioned in case of FTIR analysis of automotive coatings for forensic purposes [20, 64]. These results of outdoor weathering test in an industrial area are also the conclusive approve of the superior chemical resistance of acrylic polyurethane clearcoats, which was depicted in literature [3, 19].

CONCLUSIONS

The performance of the outdoor weathering exposure of the commercial automotive acrylic polyurethane topcoat in the industrial area (Police, Poland) was studied using both chemical (XPS, FTIR) and morphological analysis as well as gloss measurements.

The morphology characterization of the investigated clearcoat demonstrated that after the 16-month environmental weathering the coating surfaces become rough and protuberant spots of various sizes appeared. According to the results of surface chemical analyses of the exposed coatings (the XPS and FTIR methods), no evidences of polyurethane cross links degradation were noted. Finally, the features observed on the samples surfaces (after the exposure) were identified as atmospheric deposits consisting mainly of oxygen, calcium, phosphorus, iron, and silicon compounds and elemental carbon. The further results indicated that the mentioned surface contaminants may be removed from the exposed samples

by a car detailing cleaning method, which is commonly used in commercial car washes.

REFERENCES

[1] Florjanczyk Z., Penczek S.: „Chemia polimerów, tom II, Podstawowe polimery syntetyczne i ich zastosowania", Oficyna Wydawnicza Politechniki Warszawskiej, Warszawa 1997, str. 75.

[2] Tator K.B.: "ASM Handbook, Volume 5B: Protective Organic Coatings", ASM International, Ohio, United States 2015, str. 462.

[3] Streitberger H.J., Dössel K.F.: "Automotive Paints and Coatings", Willey-VCH Verlag Gmbh & Co. KGaA Wienheim, 2008, str. 175.

[4] Akafuah N.K., Poozesh S., Salaimeh A. *et al*.: *Coatings* **2016**, *6*, 24. https://doi.org/10.3390/coatings6020024

[5] Jones F.N., Nichols M.E., Pappas S.P.: "Organic Coatings: Science and Technology", Fourth Edition, John Wiley & Sons, Inc. 2017, str. 419.

[6] Głuszko M.: *Ochrona przed korozją* **2008**, *4–5*, 212.

[7] Kotnarowska D., Sirak M.: *Ochrona przed korozją* **2017**, *60*(*9*), 300. https://doi.org/10.15199/40/2017.9.2

[8] Schulz U., Trubiroha P., Schernau U. *et al*.: *Progress in Organic Coatings* **2000**, *40*, 151.

[9] Wolff G.T., Rodgers W.R., Collins D.C. *et al*.: *Journal of the Air & Waste Management Association* **1990**, *40*, 1638. https://doi.org/10.1080/10473289.1990.10466810

[10] Rezaei M., Yari H., Amrollahi S. *et al*.: *Progress in Organic Coatings* **2019**, *136*, 105193. https://doi.org/10.1016/j.porgcoat.2019.06.040

[11] Ramezanzadeh B., Mohseni M., Yari H.: *Journal of Coatings Technology Research* **2011**, *8*(*3*), 375. https://doi.org/10.1007/s11998-010-9312-z

[12] Ramezanzadeh B., Mohseni M., Yari H. *et al*.: *Progress in Organic Coatings* **2009**, *66*, 149. https://doi.org/10.1016/j.porgcoat.2009.06.010

[13] Ramezanzadeh B., Mohseni M., Yari H.: *Journal of Polymers and the Environment* **2010**, *18*, 545. https://doi.org/10.1007/s10924-010-0201-4

[14] Stevani C.V., De Faria D.L.A., Porto J.S. *et al*.: *Polymer Degradation and Stability* **2000**, *68*, 61. https://doi.org/10.1016/s0141-3910(99)00165-2

[15] Deflorian F., Rossi S., Fedrizzi L. *et al*.: *Progress in Organic Coatings* **2007**, *59*, 244. https://doi.org/10.1016/j.porgcoat.2006.09.036

[16] Gauda K.: *Postępy Nauki i Techniki* **2012**, *15*, 170.

[17] Almeida E., Alves I.N.: *Progress in Organic Coatings* **2003**, *46*(*1*) 8. https://doi.org/10.1016/S0300-9440(02)00144-3

[18] Merlatti C., Perrin F.X., Aragon E. *et al*.: *Polymer Degradation and Stability* **2008**, *93*, 896. https://doi.org/10.1016/j.polymdegradstab.2008.02.008

[19] Wernstàhl K. M.: *Polymer Degradation and Stability* **1996**, *54*, 57.

[20] Van der Pal K. J., Sauzier G., Maric M. *et al*.: *Talanta* **2016**, *148*, 715. http://dx.doi.org/10.1016/j.talanta.2015.08.058

[21] Kotnarowska D.: *Przemysł Chemiczny* **2019**, *98*, 1335. https://doi.org/10.15199/62.2019.8.26

[22] Białomazur M., Jasińska I., Krowicka, M. *et al*.: *Przemysł Chemiczny* **2020**, *99*, 892. https://doi.org/10.15199/62.2020.6.12

[23] Kottek M., Grieser J., Beck C. *et al*.: *Meteorologische Zeitschrift* **2006**, *15*/*3*, 259. https://doi.org/10.1127/0941-2948/2006/0130

[24] Gauda K., Pasierbiewicz K.: *Informatyka Automatyka Pomiary w Gospodarce i Ochronie Środowiska* **2019**, *4*, 22. https://doi.org/10.35784/IAPGOS.124

[25] Nguyen T.V., Le X.H., Dao P.H. *et al*.: *Progress in Organic Coatings* **2018**, *124*, 137. https://doi.org/10.1016/j.porgcoat.2018.08.013

[26] Mishra A.K., Chattopadhyay D.K., Sreedhar B. *et al*.: *Progress in Organic Coatings* **2006**, *55*, 231. https://doi.org/10.1016/j.porgcoat.2005.11.007

[27] Halim F.S.A., Chandren S., Nur H.: *Progress in Organic Coatings* **2020**, *147*, 105782. https://doi.org/10.1016/j.porgcoat.2020.105782

[28] Al-Turaif H.A.: *Progress in Organic Coatings* **2013**, *76*, 677. https://doi.org/10.1016/j.porgcoat.2012.12.010

[29] Che K., Lyu P., Wan F. *et al*.: *Materials* **2019**, *12*, 3636. https://doi.org/10.3390/ma12213636.

[30] Gómez-Magallón J.L., Menchaca-Rivera J.A., Pineda-Piñóna J. *et al*.: *Progress in Organic Coatings* **2020**, *147*, 105735. https://doi.org/10.1016/j.porgcoat.2020.105735

[31] Moulder J.F., Stickle W.F., Sobol P.E., Bomben K.D.: "Handbook of X-ray Photoelectron Spectroscopy", Perkin-Elmer Corporation, City of Eden Prairie USA, 1992, str. 9.

[32] Horgnies M., Darque-Ceretti E., Combarieu R.: Progress in Organic Coatings 2003. 47, 154. https://doi.org/10.1016/S0300-9440(03)00123-1

[33] Kotnarowska D.: *Progress in Organic Coatings* **2010**, *67*, 324. https://doi.org/10.1016/j.porgcoat.2009.10.026

[34] Tougaard, S. M.: " X-ray Photoelectron Spectroscopy-Elsevier Reference Module in Chemistry", Molecular Sciences and Chemical Engineering. In J. Reedijk (Ed.), Elsevier Reference Module in Chemistry, Molecular Sciences and Chemical Engineering Elsevier, 2013, str. 7. https://doi.org/10.1016/B978-0-12-409547-2.00527-8

[35] Solís-Gómez A., Neira-Velázquez M.G., Morales J. *et al*.: *Colloids and Surfaces A Physicochemical and Engineering Aspects* **2014**, *451*, 66. https://doi.org/10.1016/j.colsurfa.2014.03.021

[36] Ilango N.K., Gujar P., Nagesh A.K. *et al*.: *Cement and Concrete Composites* **2021**, *115*, 103856. https://doi.org/10.1016/j.cemconcomp.2020.103856

[37] Briggs D., Seah M.P.: "Practical Surface analysis", Chichester : Wiley, New York, 1992, str. 635.

[38] Dı́az J., Paolicelli G., Ferrer S. *et al*.: *Physical review. B, Condensed matter* **1996**, *54*, 8064. https://doi.org/10.1103/PhysRevB.54.8064
[39] Atzei D., Fantauzzi M., Rossi A. *et al*.: *Applied Surface Science* **2014**, *307*, 120. DOI:10.1016/j.apsusc.2014.03.178
[40] González L.T., Longoria-Rodríguez F.E., Sánchez-Domínguez M. *et al*.: *Journal of Environmental Sciences* **2018**, *74*, 32. https://doi.org/10.1016/j.jes.2018.02.002.
[41] Liu Y., Liu G., Yousaf B. *et al*.: *Ecotoxicology and Environmental Safety* **2020**, *202*, 110888. https://doi.org/10.1016/j.ecoenv.2020.110888
[42] Song J., Peng P.: *Aerosol Science and Technology* **2009**, *43*, 1230. https://doi.org/10.1080/02786820903325394
[43] Kelemen S.R., Afeworki M., Gorbaty M.L. *et al*.: *Energy Fuels* **2002**, *16*, 1507. https://doi.org/10.1021/ef0200828
[44] Zhang Y., Maxted J., Barber A. *et al*.: *Polymer Degradation and Stability* **2013**, *98*, 527. https://doi.org/10.1016/j.polymdegradstab.2012.12.003
[45] Zhang Y.: "Thesis: a spectroscopic study of the degradation of polyurethane coil coatings". London, UK: Queen Mary, University of London, 2012, str. 24.
[46] Maric M.: "Chemical Characterisation and Classification of Forensic Trace Evidence", PHD thesis, Curtin University, 2014, str. 14.
[47] Perrin F.X., Irigoyen M., Aragon E. *et al*.: *Polymer Degradation and Stability* **2000**, *70*, 469. https://doi.org/10.1016/s0141-3910(00)00143-9
[48] Gao T., He Z., Hihara L.H. *et al*.: *Progress in Organic Coatings* **2019**, *130*, 44. https://doi.org/10.1016/j.porgcoat.2019.01.046
[49] Thomas J., Singh V., Jain R.: *Progress in Organic Coatings* **2020**, *145*, 105677. https://doi.org/10.1016/j.porgcoat.2020.105677
[50] Kha K.: "Appearance and spectroscopic characterization of automotive coatings for forensic purposes - a Thesis", the Faculty of California Polytechnic State University, 2017, str. 37.
[51] Nguyen T.V., Nguyen Tri P., Nguyen T.D. *et al*.: *Polymer Degradation and Stability* **2016**, *128*, 65. https://doi.org/10.1016/j.polymdegradstab.2016.03.002
[52] Kumano N., Mori K., Kato M. *et al*.: *Progress in Organic Coatings* **2019**, *135*, 574. https://doi.org/10.1016/j.porgcoat.2019.06.034
[53] Di Crescenzo M.M., Zendri E., Sánchez-Pons M. *et al*.: *Polymer Degradation and Stability* **2014**, *107*, 285. https://doi.org/10.1016/j.polymdegradstab.2013.12.034
[54] Gomes de Oliveira A.G., Wiercigroch E., De Andrade Gomes J. *et al*.: *The Royal Society of Chemistry* **2018**, *10*, 1203. https://doi.org/10.1039/C7AY02684F
[55] Zięba-Palus J., Trzcińnska B.M.: *Journal of Forensic Sciences* **2013**, *58*(*5*), 1359. https://doi.org/10.1111/1556-4029.12183
[56] Gerlock J.L., Smith C.A., Cooper V.A. *et al*.: *Polymer Degradation and Stability* **1998**, *62*, 225. https://doi.org/10.1016/S0141-3910(97)00279-6
[57] Palacio S., Aitkenhead M., Escudero A. *et al*.: *PLOS ONE* **2014**, *9*(*9*), 107285. https://doi.org/10.1371/journal.pone.0107285
[58] Varrica D., Tamburo E., Vultaggio M. *et al*.: *International Journal of Environmental Research and Public Health* **2019**, *16*, 2507. https://doi.org/10.3390/ijerph16142507
[59] Roonas P., Holmgren A.: *Journal of Colloid and Interface Science* **2009**, *333*, 27. https://doi.org/10.1016/j.jcis.2008.12.080
[60] Lumetta G.J., Braley J.C., Peterson J.M. *et al*.: *Environmental Science & Technology* **2012**, *46*, 6190. https://doi.org/10.1021/es300443a
[61] Allen D.T.; Palen, E.J.; Haimov, M.I. *et al*.: *Aerosol Science and Technology* **1994**, *21*, 325. https://doi.org/10.1080/02786829408959719
[62] Madejová J., Komadel P.: *Clays and Clay Minerals* **2001**, *49*, 410. https://doi.org/10.1346/CCMN.2001.0490508
[63] Ragosta G., Abbate M., Musto P.: *Polymer* **2005**, *46*, 10506. https://doi.org/10.1016/j.polymer.2005.08.028
[64] International Standard Guide for Forensic Paint Analysis and Comparison, ASTM E1610-02 (2008), ASTM, West Conshohocken, PA, 2005.

Received 14 IX 2021.